ELSEVIER

Ceramics International 28 (2002) 887–892

CERAMICS INTERNATIONAL

www.elsevier.com/locate/ceramint

# Kinetic investigation of the carbothermal reduction of an Iranian clay

Cavus Falamaki*, Touradj Ebadzadeh

*Ceramics Department, Materials and Energy Research Center, PO Box 14155-4777, Tehran, Iran*

Received 15 January 2002; received in revised form 2 February 2002; accepted 25 March 2002

**Abstract**

The kinetics of the carbothermal reduction of clay under argon atmosphere has been investigated by the X-ray diffraction method. The clay-carbon (excess) mixture was formed into 2 cm diameter disks of different thicknesses. Experimental data evidences the significant effect of sample thickness on the reaction rate at 1400 °C. Decreasing thickness promotes mullite dissociation and formation of SiC and alumina powders. Mathematical modeling of the reaction system showed the gas diffusion in the Knudsen regime through the pellet to be the rate controlling step. Diffusivity of CO and reacted core tortuosity factor have been calculated.


*Keywords:* A. Powders: solid state reaction; B. X-ray methods; D. Clays; E. Refractories

## 1. Introduction

The carbothermal reduction of clay is an economical route to the production of $Al_2O_3$–SiC mixtures. $Al_2O_3$–SiC–C refractory has a good erosion and spallation resistance and is durable against oxidizing attack at elevated temperatures [1]. Because of attractive mechanical properties, $Al_2O_3$–SiC composites have been used in, or being considered for use in harsh applications such as cutting tools and advanced heat engines [2–3].

The carbothermal reduction of clay proceeds through the following reaction [4]:

$$Al_2O_3.2SiO_2.2H_2O_{(s)} + 2C_{(s)} \rightarrow Al_2O_{3(s)} + 2SiO_{(g)} + 2CO_{(g)} + 2H_2O_{(g)} \quad (a)$$

The source of clay in reaction (a) is kaolin. If excess carbon is supplied, SiO may take part in the following reduction reaction [5]:

$$SiO_{(g)} + 2C \rightarrow SiC_{(s)} + CO_{(g)} \quad (b)$$

Therefore, the transformation of clay into $Al_2O_3$–SiC involves many reactions and transport phenomena. Rate limiting steps in the carbothermal reduction of kaolin to β′-sialon using a packed bed reactor under nitrogen atmosphere have been discussed by Van Dijen et al. [6]. They found out that specific area of powder, catalytic effect of impurities and gas diffusion through the pellets may all act as rate controlling parameters. Bechtold and Cutler [4] performed kinetic experiments for the reaction of clay and carbon to form separate $Al_2O_3$–SiC particles. They used a dispersion of crushed clay–carbon mixture pellet within a carbon black matrix. The whole was in the form of pellets. Their work lacks of the determination of reaction rate constants and mass transfer parameters, like CO diffusivity through the clay–carbon pellet.

Considering the gaseous products of reactions (a) and (b), it is obvious that the pellet should be as compact as possible in order to increase the carbon–mullite interface and avoid SiO escaping out of the pellet. On the other hand, low porosity and poor communication between pores prevents CO to exit the pellet affecting adversely the $Al_2O_3$ and SiC formation.

The present work treats pellets of the clay–carbon mixtures containing excess carbon in order to induce complete SiO reduction into SiC. The authors of the present work do not intend to produce separate $Al_2O_3$ and SiC. Instead, they aim at the production of $Al_2O_3$–SiC

* Corresponding author. Fax: +98-21-877-3352.
*E-mail address:* c-falamaki@merc.ac.ir (C. Falamaki).

0272-8842/02/$22.00 
PII: S0272-8842(02)00069-X

mixtures to be implemented in the manufacture of refractory.

The phase development is followed and quantified using the XRD technique. The rate limiting steps are discussed and the CO diffusivity is calculated.

## 2. Experimental

The starting materials were carbon black with a specific surface area of 106 $m^2\ g^{-1}$ and graphite with particle sizes 95% lower than 35 μm as carbon sources and Iranian kaolin (Zenouz) as clay source. The chemical analysis of the latter is shown in Table 1. The starting powders were dry mixed in a ball mill for 2 h with alumina grinding medium to a sample charge weight ratio of 3:1. The batch composition had been 20% carbon black, 15% graphite and 65% clay, on a mass basis. The 1, 2 and 3 g mixed powders were uniaxially pressed in a steel die with 20 mm diameter at 30, 60 and 90 MPa, respectively. The samples had a thickness of 1.95, 3.25 and 4.6 mm, respectively. The heating regimes were carried out in a controlled atmosphere tube furnace at 1400 °C . The latter was chosen so as to avoid reduction of $Al_2O_3$ and, at the same time, resulting in appreciably high reaction rates. The compacts were heated up to the reaction temperature with a constant rate of 10 °C $min^{-1}$ . The Ar flow rate was kept constant for all runs at 2 l $min^{-1}$. The bulk density was determined by weighing the pressed powders and dividing by the bulk volume calculated from the sample dimensions. The crushed samples were heated at 700 °C for 4 h to remove the remaining carbon. The heated samples were then analyzed by the X-ray diffraction technique using a D-500 (Siemens) diffractometer with Cu$K_\alpha$ radiation. The mullite phase of the reacted samples was quantitatively analyzed by the XRD technique. A calibration curve relating the $SiC/(SiC + Al_2O_3)$ mass ratio to $\Sigma I_{SiC}/(\Sigma I_{SiC} + \Sigma I_{Al_2O_3})$ peaks intensity ratio was constructed. For this means, the planes (110), (120) and (210) for orthorhombic mullite, (012), (110), (113) and (024) for α-alumina and (111) and (200) for cubic silicon carbide were used for quantitative analysis. Specific area determination was performed by the BET technique (Micromeritics).

Table 1
Chemical analysis of the clay used in this work

| Compound name | Wt.% |
|---|---|
| $SiO_2$ | 48.46 |
| $Al_2O_3$ | 39.22 |
| $Fe_2O_3$ | 0.20 |
| $TiO_2$ | 0.25 |
| CaO | 0.50 |
| MgO | 0.30 |
| $K_2O$ | 1.10 |
| L.O.I. | 9.97 |

## 3. Results and discussion

### 3.1. Phase evolution

Figs. 1 and 2 show the X-ray pattern of the samples with the smallest thickness (1.95 mm) and largest thickness(4.6 mm) processed for different times. The thick sample heated for 4.2 min exhibits sharp SiC peaks while alumina peaks can hardly be detected. Actually, kaolin is first dehydroxylated and then transformed into metakaolin at temperatures lower than 1000 °C. The latter dissociates into mullite and silica before reaching the main reaction temperature. Small amount of impurities and structural defects in the clay minerals promote the distortion of the atomic structure as well as forming a liquid phase (mainly amorphouse silica) at the high firing temperature employed. In this respect, based on the formation of liquid phase and cristobalite during transformation of clay into mullite, it seems very probable that SiC is formed prior the dissociation of mullite and formation of alumina particles. On the other hand, the initial clay contained quartz and muskovite phase impurities. These impurities are reduced to SiC, eventually before mullite dissociation. According to the calibration curve shown in Fig. 3, mullite does not affect

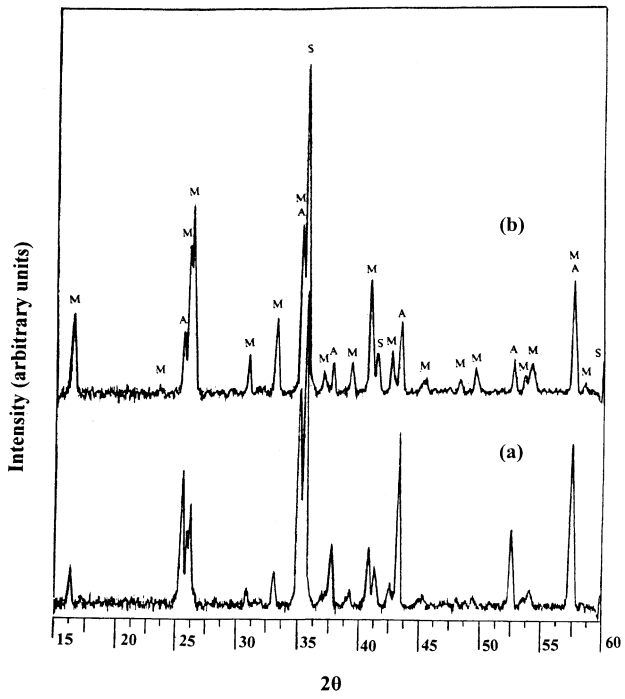


Fig. 1. XRD pattern of the sample of 1.95 mm thickness (a) after 34.0 min and, (b) after 4.2 min. A, M and S symbols stand for alumina, mullite and silicon carbide, respectively.

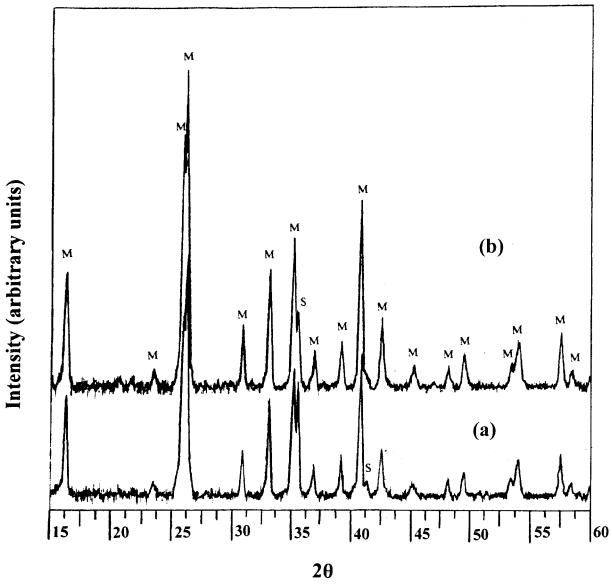


Fig. 2. XRD pattern of the sample of 4.6 mm thickness (a) after 34.0 min and, (b) after 4.2 min. A, M and S symbols stand for alumina, mullite and silicon carbide, respectively.

significantly the $SiC/(SiC+Al_2O_3)$ mass ratio in mixtures consisting of constant particle size distribution of each of the components. However, referring to Fig. 4, the latter ratio variation with time of reaction is not reasonable. During the reaction, it is presumed that the cited ratio is lower or equal to the final value (theoretically about 0.44). It could be further postulated that the formed alumina particles could not be detected by X-ray technique due to the very small size of the particles during the early stage of formation. The thinner the reacting system, the more the observed $SiC/(SiC+Al_2O_3)$ mass ratio approaches its theoretical value during the reaction. This may be attributed to a faster mullite dissociation reaction resulting in a faster growth of alumina particles. Fig. 5 shows clearly the effect of sample thickness on the reduction reaction rate

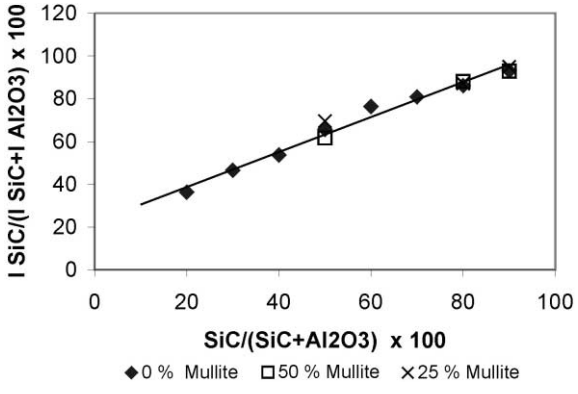


Fig. 3. Calibration curve showing $\Sigma I_{SiC}/(\Sigma I_{SiC}+\Sigma I_{Al_2O_3})$ peaks intensity ratio versus $SiC/(SiC+Al_2O_3)$ mass ratio relationship for different mullite concentrations.

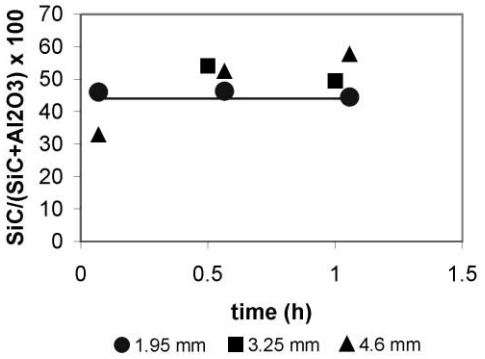


Fig. 4. $SiC/(SiC+Al_2O_3)$ mass ratio as a function of thickness and time calculated using the calibration curve of Fig. 3. The straight line corresponds to the theoretical value.

of mullite and formation of SiC and alumina phases. Increasing the thickness of the samples from 1.95 to 4.6 mm significantly prohibits the reduction reaction of mullite. Presumably, these results are consistent with the fact that the diffusion of CO gas formed from reaction between $SiO_2$ and C is encountered with difficulty by increasing the sample thickness. Such a result has been reached by Krstic [7] for the carbothermal reduction of SiC. The latter reaction is highly endothermic up to 1500 °C and, unless the CO gas produced is removed, a high overall temperature is needed to achieve a reasonable rate.

### 3.2. Determination of the rate controlling step

The reaction system involves an irreversible heterogeneous reaction of the shrinking core or topochemical model. According to the typical cylindrical geometry of the pellets under study (for which $L << D$), a one-dimensional approach is proposed. Fig. 6 shows a schematic representation of the reaction system. Two diffusional resistances act in series; diffusion of CO through the reacted inner core to the pellet outer surface and diffusion from the outer surface to the bulk carrier gas (argon). The high carrier gas flow rate employed (2 l $min^{-1}$) is presumed to cancel out the latter diffusional resistance. On the other hand, the pellet is considered to be isothermal. With these assumptions it may be shown that the relationship between the fraction of unreacted mullite and time is as follows (see Appendix):

$$f = 1 - \frac{1}{L}\left(5.953 \times 10^{-4} C_e D_{eff}/\rho\right)^{0.5} \quad (1)$$

where $f$ is the fraction of unreacted mullite, $L$ is half of the pellet thickness (m), $C_e$ is the equilibrium CO concentration (mole $m^{-3}$), $D_{eff}$ is the effective diffusion coefficient ($m^2$ $s^{-1}$) and $\rho$ is the density of the reacted core (g $cm^{-3}$). According to Fig. 5, Eq. (1) reasonably

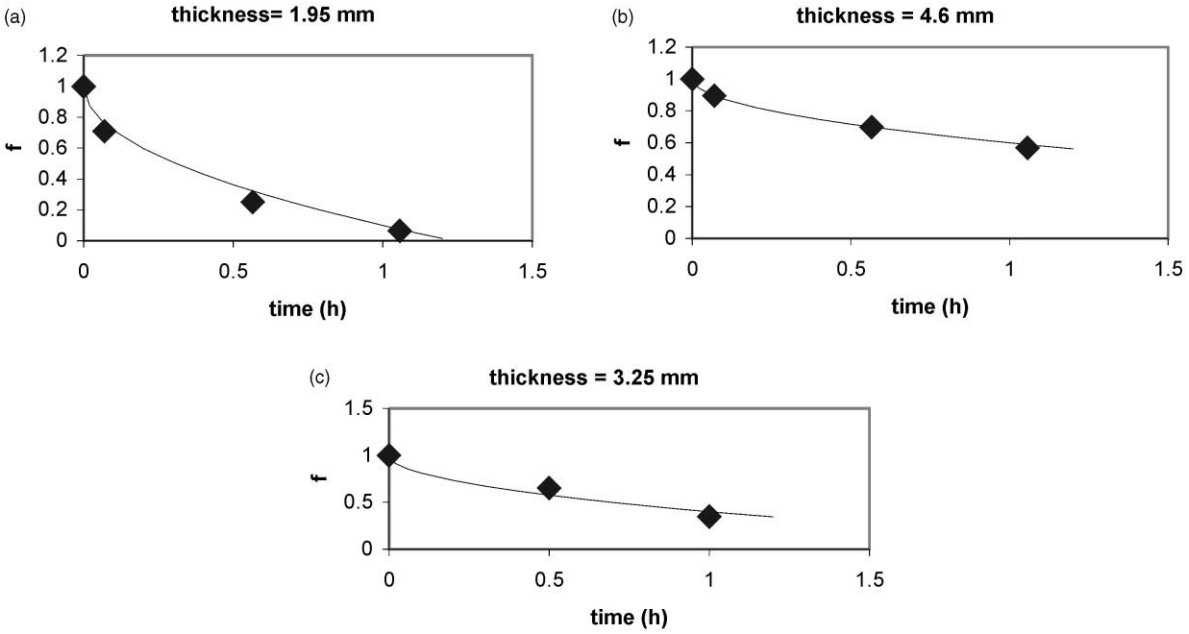


Fig. 5. Mullite conversion into SiC and $Al_2O_3$ as a function of time for different thicknesses.

predicts the experimental data for the three thicknesses under study. As observed, increasing the thickness of the samples slows down the reduction reaction rate of mullite.

X-ray analysis showed that at zero reaction time, all initial kaolin had been completely transformed into mullite. The overall reaction describing the transformation of mullite into SiC and $Al_2O_3$ is as follows:

$$Al_6Si_2O_{13(s)} + 6C_{(s)} \rightarrow 3\ Al_2O_{3(s)} + 2SiC + 4CO_{(g)} \quad (c)$$

If the rate-controlling step is the mass diffusion through the reacted outer layer, reaction (c) may be considered to be at equilibrium at the reacted–unreacted core interface. The free energy change of reaction (c) at 1400 °C may be calculated using available thermodynamic data (H, S, $C_p$) for each of the species involved [8]. Thus we get:

$$\Delta G^{1400^\circ C} = 82\ 767.51\ \text{J mol}^{-1} \quad (2)$$

The concentration of CO is then evaluated assuming unity activity for the solid species involved:

$$C_e = C_{CO} = \frac{1}{RT}\left(e^{\frac{-\Delta G}{RT}}\right)^{\frac{1}{4}} = 1.624 \times 10^{-5}\ \text{mol m}^{-3} \quad (3)$$

where $C_{CO}$ is the equilibrium CO concentration (mol $m^{-3}$), $R$ is the universal gas constant and $T$ is the reaction temperature (K). Table 2 summarizes density and porosity data of the samples prior and after the carbothermal treatment. Introducing the pertaining values in Eq. (1), the effective diffusion coefficient for the thin, medium and thick samples are evaluated to be 0.01944, 0.02539 and 0.0231 $m^2\ s^{-1}$, respectively. The difference in the diffusivity is attributed to the difference in initial density of the samples and as a consequence, to the different tortuosities. The obtained results sustain the initial hypothesis that gas diffusion through the pellet is the rate-controlling step.

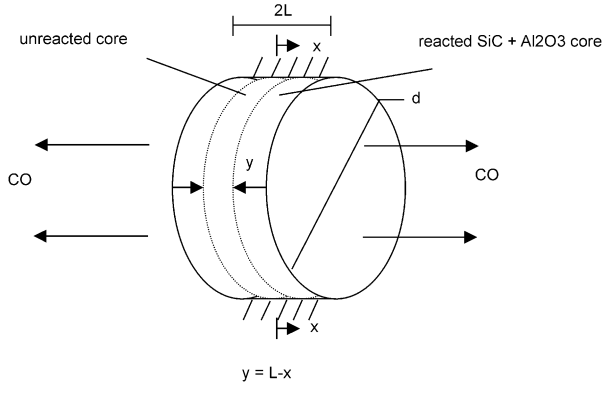


Fig. 6. Schematic representation of the reacting system.

### 3.3. Determination of the diffusion mechanism

To elucidate the diffusion mechanism involved, the specific surface area of the thick sample prior and after reaction had been measured to be 28.2 and 17.6 $m^2\ g^{-1}$, respectively. Applying the following relation:

Table 2
Bulk density and porosity of samples before and after heating at 1400 °C

| Sample thickness (mm) | Before heating | | After heating | |
|---|---|---|---|---|
| | Density (g cm$^{-3}$) | Porosity (%) | Density (g cm$^{-3}$) | Porosity (%) |
| 4.60 | 1.26 | 47.28 | 0.95 | 60.25 |
| 3.25 | 1.21 | 49.37 | 0.93 | 61.09 |
| 1.95 | 1.01 | 57.7 | 0.88 | 63.18 |

$$d = \frac{4\varepsilon}{S\rho} \tag{4}$$

where $d$ is the reacted pore diameter (m), $\varepsilon$ is the porosity of the reacted core and $S$ is the specific area (m$^2$ g$^{-1}$), the pore diameter of the reacted outer core is calculated to be $1.44\times10^{-7}$ m. Applying the following equation:

$$D_k = 48.5d\sqrt{T}/M \tag{5}$$

where $D_k$ is the Knudsen diffusion coefficient (m$^2$ s$^{-1}$) and $M$ is the gas molecular weight (g mol$^{-1}$), the Knudsen diffusivity is evaluated to be 0.1021 m$^2$ s$^{-1}$. The molecular diffusivity, $D_m$, may be calculated using the Chapman–Enskog theory [9]:

$$D_m = \frac{1.86\times10^{-3}T^{1.5}\left(\frac{1}{M_{CO}}+\frac{1}{M_{Ar}}\right)}{p\sigma_{12}^2\Omega} \tag{6}$$

where $p$ is the total pressure (atm), $\sigma_{12}$ is the collision diameter (Å) and $\Omega$ is the collision integral. For the CO–Ar binary system, $\sigma_{12}=3.616$ Å and $\Omega=0.9594$. Thereof, $D_m$ is evaluated to be 0.616 m$^2$ s$^{-1}$. It is observed that $D_{eff}<D_k<D_m$. Hence, the diffusion mechanism is of the Knudsen type through the tortuous pathways of the reacted core. Considering the following [10]:

$$\frac{\tau}{\delta} = \frac{\left(\frac{1}{D_k}+\frac{1}{D_m}\right)^{-1}\varepsilon}{D_{eff}} \tag{7}$$

where $\tau/\delta$ is the tortuosity ratio, $\tau$ is the tortuosity and $\delta$ is the constriction factor, the tortuosity factor of the thick sample is evaluated to be 2.284. Considering a typical constriction factor $\delta$ of 0.8, the tortuosity is calculated to be 2.855. Tortuosities usually range between two and six, averaging about 3 [11].

## 4. Conclusions

The solid state carbothermal reduction of an Iranian commercial kaoline has been investigated. For the pellet geometry and the high argon gas Reynolds number (Re = 416) employed, it had been shown that Knudsen diffusion of CO through the pellet is the rate controlling step. Therefore the thinner the pellet, the higher the reaction rate of mullite into $Al_2O_3$ and SiC transformation. Although a lower initial green compact density promotes this reaction, it may also lead to the premature escape of SiO and, as a consequence, less SiC yield. The authors of this work suppose that it is necessary to optimize initial pellet thickness versus initial pellet density.

The results of this study may be implemented in the industrial scale production of $Al_2O_3$–SiC mixtures as refractory raw materials. For this means and based on some preliminary results, the authors of this work suppose that it is worth to investigate the reaction under air atmosphere. In the latter case the use of the expensive Ar gas might be substituted with compressed air.

## Appendix

The mass balance over the two growing cylindrical elements as shown in Fig. 6 is written as:

$$4\frac{dm}{dt} = -2Ak(C_{in}-C_s)y \tag{8}$$

where $m$ stands for moles mullite of the growing cylindrical elements (g mol$^{-1}$), $t$ is time (h), $A$ is the pellet surface perpendicular to CO flow (m$^2$), $k$ is the mass transfer coefficient (taken equal to $D_{eff}$/y, m s$^{-1}$), $y$ is the coordinate in Fig. 6, $C_{in}$ is the CO concentration at the reacted-unreacted core interface (mol m$^{-3}$) and $C_s$ is the CO concentration at the outer pellet surface (mol m$^{-3}$). The factor 4 in the left hand term is due to 4 mol CO produced per each mole mullite reacted. The left hand term is equal to the negative of the rate of CO diffusion through the reacted core. As the external diffusion occurs relatively fast, the value of $C_s$ can be reasonably taken as zero. On the other hand:

$$m = A.2y.\rho.\beta \tag{9}$$

where $\beta$ is the pertaining conversion factor ($\beta = 839.7932$). Introducing Eq. (8) in (7) and integrating, Eq. (1) is obtained.

## References

[1] K. Takeda, K. Yuki, US Patent 3 753 744, 1973.
[2] P.F. Becher, G.C. Wei, Toughening behavior in SiC-whisker-reinforced alumina, J. Am. Ceram. Soc. 67 (1984) c267–c269.
[3] G.C. Wei, P.F. Becher, Development of SiC-whisker-reinforced ceramics, Am. Ceram. Soc. Bull. 64 (1985) 298–304.
[4] B.C. Bechtold, I.B. Cutler, Reaction of clay and carbon to form and separate $Al_2O_3$ and SiC, J. Am. Ceram. Soc. 63 (5–6) (1980) 271–275.
[5] J.G. Lee, Carbide and nitride ceramics by carbothermal reduction of silica, Univ. Microfilms Int. (Ann Arbor Mich.), Order No. 76–19955, 102 pp, Diss. Abstr. Int B. 37 (7) (1976) 1379.
[6] F.K. Van Dijen, R. Metselaar, C.A.M. Siskens, Reaction-rate-limiting steps in carbothermal reduction processes, J. Am. Ceram. Soc. 68 (1) (1985) 16–19.
[7] V.D. Krstic, Production of fine, high-purity beta silicon carbide powders, J. Am. Ceram. Soc. 75 (1) (1992) 170–174.
[8] O. Kubaschewski, C.B. Alcock, P.J. Spencer, Materials Thermochemistry, Pergamon Press, 1993, pp. 257–323.
[9] E.L. Cussler, Diffusion, Mass Transfer in Fluid Systems, Cambridge University Press, 1997, p. 104.
[10] J M. Smith, Chemical Engineering Kinetics, McGraw Hill, 1981, p. 468.
[11] Reference 9, p. 173.